# Thermomechanical Fatigue Behavior and Lifetime Prediction of Niobium-added Ferritic Stainless Steel

J.G. Jung[1], Y.J. Oh[2], W.D. Choi[2], W.J. Yang[3]
[1]*Hyundai Motors Inc., Hwaseong, S. Korea;*
[2]*Hanbat University, Daejon, S. Korea;*
[3]*Korea Inst. of Materials Science, Changwon, S. Korea*
E-mail: *yongjun5@gmail.com*

Abstracts

Thermomechanical fatigue (TMF) and isothermal fatigue (IF) behaviors of niobium-added ferritic stainless steel were presented in the temperature range from 100 °C to 800 °C; further, we proposed a new fatigue failure criterion to predict the lifetimes of the components for different thermal cycle ranges in the TMF condition. The test results revealed that the TMF life decreased monotonously as the maximum temperature increased higher than 600 °C. By modifying the Coffin-Manson equation using the temperature factor, we obtained a new parameter that was successfully correlated with the lifetime under a different maximum temperature. The stress-strain hysteresis loops and cyclic stress responses during fatigue cycling were compared to elucidate the different fatigue behaviors under TMF and IF conditions.

## 1. Introduction

Thermomechanical fatigue (TMF) is one of the key life-limiting factors affecting engineering components operating at high temperature. Among the components in automotive technology, exhaust manifolds, the part that connects the high-temperature exhaust gas from the engine to the exhaust pipe, are especially prone to TMF failure due to severe thermal gradients during start-stop cycles [1,2]. To predict the failure location and endurance lifetime of the component, fatigue data of the materials are needed. Isothermal low-cycle-fatigue (IF) data evaluated at elevated temperatures have been traditionally used due to the convenience of the testing method, instead of TMF. However, several researchers have indicated that there is a large discrepancy between the lifetimes under TMF and IF loading conditions as material and exposure temperatures vary [3,4]. Since the heat-resistant ferritic stainless steels used for exhaust manifolds show a dramatic reduction in tensile property at the temperature range of >600 °C [5], a comparison of IF and TMF behaviors in the temperature range can be a primary concern for higher temperature application of the steels.

The aim of the present work is to evaluate IF and TMF behaviors in the operating temperature range up to 800 °C. We compare the change in the lifetime and cyclic stress-strain response under different loading conditions with variations in the testing temperature range.

## 2. Experimental procedure

The material examined here is a heat-resistant ferritic stainless steel (15 Cr-1.5 Mo) with a content of niobium 0.5 wt% to improve the high temperature strength. The chemical composition and mechanical properties at elevated temperatures are given in Table 1.

All fatigue tests described here were carried out on thin-walled cylindrical specimens, whose outer diameter was 7 mm and inside was 4 mm, using a closed loop servo-hydraulic testing machine. The specimens were heated by a high-frequency induction heating system and cooled by a controlled air jet into the specimen core and outer surface simultaneously. The heating and cooling speed of the triangular temperature cycle was 350 °C/min. The minimum temperature $T_{min}$ was 100 °C, and the maximum temperature $T_{max}$ varied between 500 °C and 800 °C. In the TMF test, the total strain range ( $\Delta\varepsilon_t$ ), which consists of mechanical ( $\Delta\varepsilon_m$ ) and thermal strain ranges ( $\Delta\varepsilon_{th}$ ), was kept constant. Under the out-of-phase (OP) TMF condition, $\Delta\varepsilon_m$ and $\Delta\varepsilon_{th}$ have opposite signs, and the restraint ratio (η) is correlated to the total strain range by the following equation:

$$\eta = -\Delta\varepsilon_m / \Delta\varepsilon_{th} \text{ , } \cdots\cdots(1)$$

where $\Delta\varepsilon_m = \Delta\varepsilon_t - \Delta\varepsilon_{th}$ .

Table 1. The chemical composition and mechanical properties of the heat-resistant ferritic stainless steel used in this study.

| C | Si | Mn | Cr | Ni | Mo | Nb |
|---|---|---|---|---|---|---|
| 0.002 | 0.360 | 0.203 | 15.07 | 0.212 | 1.520 | 0.530 |

| Temp. ( °C) | Yield strength (MPa) | Tensile strength (MPa) | U. Elongation (%) |
|---|---|---|---|
| RT | 337 | 487 | 19.5 |
| 400 | 208 | 418 | 23.0 |
| 600 | 166 | 376 | 8.3 |
| 800 | 41 | 42 | 1.6 |

Transmission electron microscopy (TEM) was used to characterize the deformed microstructure and precipitates after fatigue cycling, and scanning electron microscopy (SEM) was used to observe fatigue failure.

## 3. Results and discussion

### 3.1. Cyclic stress and strain responses

The typical stress-strain hysteresis loops obtained at half of the endurance lifetime ($N_f$) are given in Fig. 1. Under the IF loading condition, the stress amplitude $\sigma_a$ decreases as the testing temperature increases. At 800 °C, the $\sigma_a$ becomes extremely low, and the loop is characterized by an almost square shape, showing no resistance against plastic deformation. On the contrary, the stress-mechanical strain hysteresis loops from the OP TMF tests are quite different from those of IF, as shown in Fig. 1(b). The tensile and compressive peak stresses ($\sigma_T$ and $\sigma_C$) decrease as $T_{max}$ increases to 600 °C. However, at $T_{max} \geq 600$ °C, the decrease in $\sigma_C$ becomes smaller whereas the decrease in $\sigma_T$ becomes bigger. At the same time, a dynamic stress relaxation of the induced compressive stress occurs during heating up $T_{max}$ after exceeding $\sigma_C$ at a certain temperature. Fig. 2 shows that the amount of the relaxation is linearly proportional to $T_{max}$.

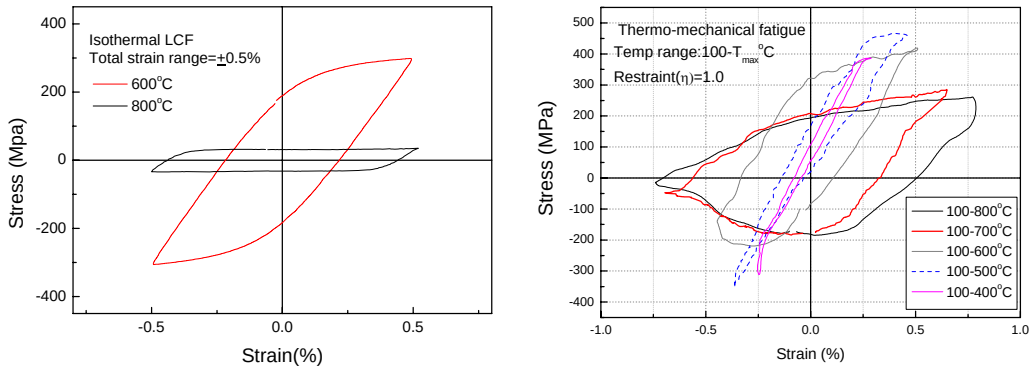


Fig. 1. Typical stress-strain hysteresis loops for (a) the IF and (b) TMF conditions.

Fig. 3 shows the development of the stress responses ($\sigma_T$ and $\sigma_C$) during the IF and OP TMF tests cycled at different $T_{isothemal}$ and $T_{max}$, respectively. The responses under IF loading are characterized by a continuous cyclic hardening at 600 °C and cyclic softening at 800 °C. Under the OP TMF loading, however, continuous cyclic hardening occurred at $T_{max}$ = 500 °C, and the response at $T_{max}$ =

600 °C exhibited a transition from initial cyclic hardening in a few tenths of a cycle into the cyclic softening up until the final failure. At $T_{max}$ > 700 °C, neither cyclic hardening nor softening was observed; constant peak stress responses were observed for all the lifetimes.

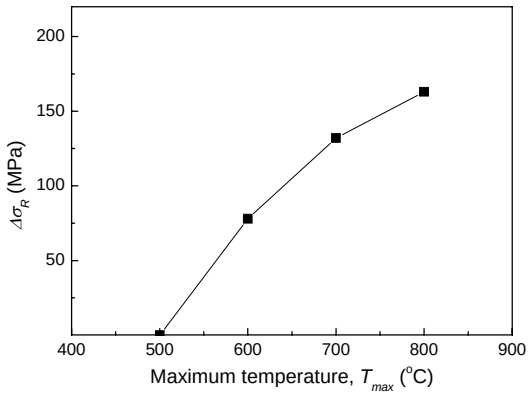


Fig. 2. The change in the dynamic stress relaxation with respect to the maximum temperature under the TMF condition.

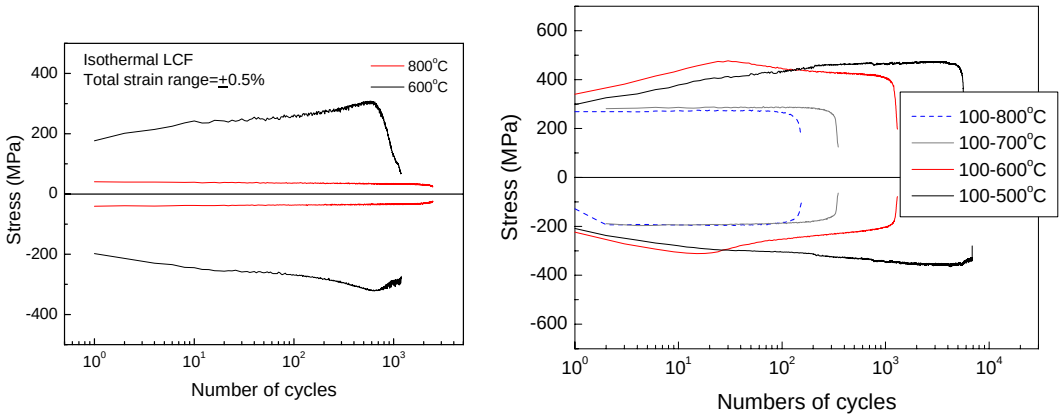


(a) (b)

Fig. 3. Peak stress responses during the (a) IF and (b) TMF cycles.

3.2. Fatigue life

Figs. 4(a) and (b) show the plots of the mechanical strain range ($\Delta\varepsilon_m$) versus the endurance lifetime ($N_f$) and the plastic strain range ($\Delta\varepsilon_p$) versus $N_f$, respectively. Under IF loading, the fatigue life at 800 °C is longer than that at 600 °C in both

figures. This extraordinary result can be understood by considering the hysteresis loops at 800 °C. As we indicated in Fig. 1, the resistance against plastic deformation as well as the absolute peak stresses during cycling was extremely low at 800 °C, similar to the elastic-perfect plastic behavior. In this condition, the material undergoes much uniform deformation, and the stress cannot be locally intensified to initiate and propagate fatigue cracks. The difference in the fracture appearances supports this; at 600 °C, the specimens exhibited distinctive crack initiation and propagation stages before the final fracture, whereas at 800 °C the wall thinning process, not crack propagation, ruptured the specimens.

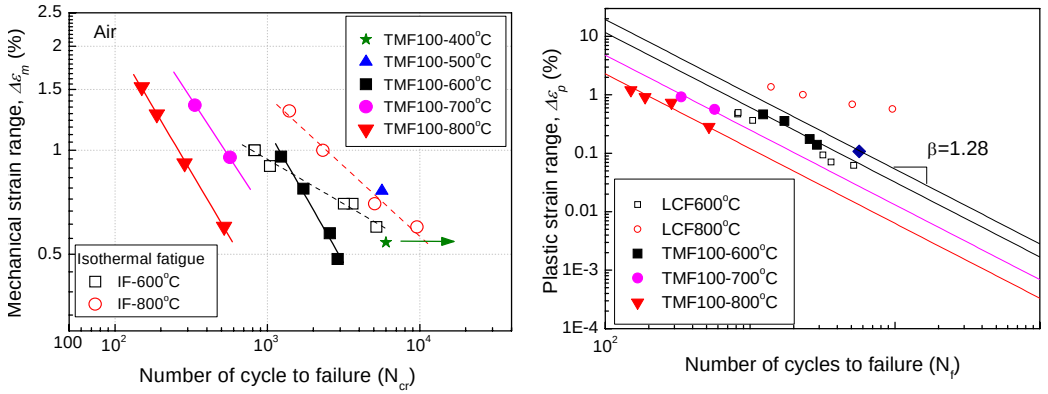


Fig. 4. (a) Mechanical strain range versus fatigue life and (b) plastic strain range versus fatigue life under IF and TMF conditions.

On the other hand, under the OP TMF loading, the fatigue life gradually decreased as $T_{max}$ increased to 800 °C. In Fig. 4(b), the $\Delta\varepsilon_p$, which was obtained from the strain range at zero stress in the hysteresis loops in Fig. 1(b), linearly correlates to the $N_f$ in the log-log plot for all temperature conditions here, satisfying the following Coffin-Manson equation:

$$\Delta\varepsilon_p \cdot N_f^{\beta} = C \quad \cdots\cdots(2)$$

where $\alpha$ and $C$ are constant. Interestingly, the constant $\beta$, which is the slope of the plots, seems to be unchanged with $T_{max}$. So, using the average value of $\beta$, we can calculate the constant C at a different $T_{max}$ from the above equation, and plot it against $T_{max}$, as shown in Fig. 5. In the figure, a good linear relationship between the log C and $T_{max}$ exists, which can be expressed by the following equation:

$$\log C = mT_{\max} + n \quad \cdots\cdots(3)$$

For the material in this study, the $m$ and $n$ were –0.00316 and 6.330, respectively. Substituting eq. (3) into eq. (2), eq. (2) is rewritten to the following unified form of the equation:

$$H_D \cdot N_f{}^{\beta} = C \quad \text{.....(4)}$$

where, $H_D = \Delta\varepsilon_p / 10^{m \cdot T_p}$ .....(5)

In Fig. 6, the temperature-modified parameter, $H_D$, which was calculated in a different $T_{max}$ and strain ranges, is plotted against the actual fatigue life, $N_f$. All data points under different conditions fit into one correlation line with small deviations.

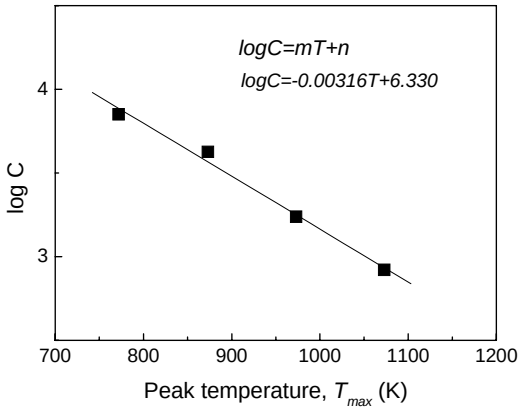


Fig. 5. The log C versus the peak temperature of the TMF cycle.

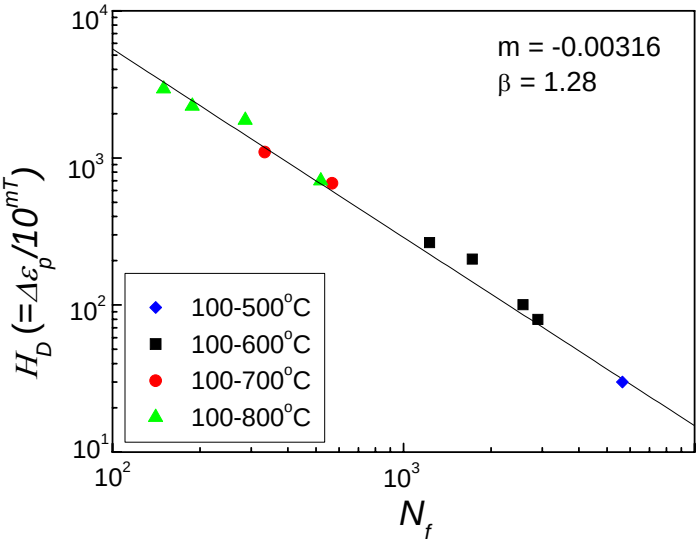


Fig. 6. The temperature-modified fatigue parameter versus the actual TMF lifetime.

The above unified equation that successfully modifies the $T_{max}$ effect is based on the meaningful relationship between C and $T_{max}$ in eq. (3). To explain that relationship, two different damage contributions can be taken into account: oxidation and stress relaxation during the high-temperature part of the loop. Indeed, oxidation can strongly accelerate the initiation and growth of fatigue cracks in the specimen's surface [6]. However, since the material exhibited a much longer life at 800 °C than at 600 °C under the IF condition, oxidation does not seem to be a decisive mechanism describing the TMF life degradation with higher $T_{max}$. The other explanation can be given by considering the stress relaxation during the heating-up half of the cycle [2]. As already shown in Fig. 2, the amount of the dynamic stress relaxation ($\Delta\sigma_R$) is proportional to $T_{max}$ at temperatures greater than 500 °C. This relaxation reduces the flow stress, and enhances local stress concentration during subsequent tensile loading (the cooling part of the loop). The relaxation during the heating-up half of the cycle can raise the mean stress during the subsequent cooling-down half of the cycle as well. The details of these mechanisms will be described in other papers.

## 4. Conclusions

The thermomechanical fatigue (TMF) and isothermal low-cycle fatigue (IF) lives of niobium-added ferritic stainless steel were evaluated. The IF test resulted in a longer life at 800 °C than at 600 °C. However, TMF life decreased with an increase in the maximum temperature above 600 °C, although the TMF life at each temperature range well correlated with the plastic strain range as a form of the Coffin-Manson equation. To obtain the unified correlation, the Coffin-Manson equation was modified by taking into account the temperature effect. The resultant new parameter successfully showed a single correlation with the lifetime tested at different temperature ranges. The physical implication involved in the proposed equation was discussed in view of the dynamic stress relaxation and cyclic stress responses during cycling.

## Acknowledgement

This work has been supported by Hyundai-Kia Motors and partly by Materials Bank Program, which is funded by MKE (Ministry of Knowledge and Economy).

## References

[1] G. Chinouilh, P.O. Santacreu, J.M. Herbelin, Thermal fatigue design of stainless steel exhaust manifolds, SAE international Conference, SAE Paper No.

2007-01-0564
[2] F. Liu, S.H. Ai, Y.C. Wang, H. Zhang, Z.G. Wang, Thermal-mechanical fatigue behavior of a cast K417 nickel-based superalloy, International Journal of Fatigue, 24 (2002) 841-846
[3] K. Rau, T. Beck, D. Lohe, Isothermal, thermal-mechanical and complex thermal-mechanical fatigue tests on AISI 316L steel-a critical evaluation, Mater. Sci. Eng. A 345 (2003) 309-318
[4] A. Miyazaki, J. Hirasawa, S. Satoh, Advanced stainless steels for stricter regulations of automotive exhaust gas, Kawasaki Steel Technical Report No. 43 Oct 2000, pp. 21-27
[5] N. Fujita, K. Ohmura, A. Yamamoto, Changes of microstructures and high temperature properties during high temperature service of niobium added ferritic stainless steels, Mater. Sci. Eng. A 351 (2003) 272-281
[6] H-J. Christ, Effect of environment on thermomechanical fatigue life, Mater. Sci. Eng. A 468-470 (2007) 98-108